A Fiducial-Aided Reconfigurable Artefact for the Estimation of Volumetric Errors of Multi-axis Ultra-Precision Machine Tools

Shixiang Wang
Fudan University
Chi Fai Cheung (Benny.Cheung@polyu.edy.hk)
Hong Kong Polytechnic University https://orcid.org/0000-0002-6066-7419
Lingbao Kong
Fudan University

Research Article

Keywords: ultra-precision machining, on-machine laser scanner, reconfigurable artefact, fiducial, volumetric errors, machine tools

Posted Date: July 6th, 2021

DOI: https://doi.org/10.21203/rs.3.rs-581329/v1

Version of Record: A version of this preprint was published at Applied Sciences on February 10th, 2022.
See the published version at https://doi.org/10.3390/app12041824.

A fiducial-aided reconfigurable artefact for the estimation of volumetric errors of multi-axis ultra-precision machine tools

Shixiang Wang[1], Chifai Cheung[2*] and Lingbao Kong[1]

1. Shanghai Engineering Research Center of Ultra-precision Optical Manufacturing, School of Information Science and Technology, Fudan University, Shanghai, China

2. State Key Laboratory of Ultra-precision Machining Technology, Department of Industrial and Systems Engineering, The Hong Kong Polytechnic University, Hung Hom, Kowloon, Hong Kong

* Correspondence: Benny.Cheung@polyu.edu.hk;

Abstract

In this paper, a fiducial-aided reconfigurable artefact is presented for estimating volumetric errors of a multi-axis machine tools. The artefact makes use of an adjustable number of standard balls as fiducials to build a 3D artefact which has been calibrated on a coordinate measuring machine (CMM). This 3D artefact shows its reconfigurability in its number of fiducials and their locations according to the characteristics of workpieces and machine tools. The developed kinematics of the machine tool was employed to identify the volumetric errors in the working space by comparing the information acquired by the on-machine metrology with that by the CMM. Experimental studies are conducted on a five-axis ultra-precision machine tools mounted with the 3D artefact composed of five standard spheres. Factors including the gravity effect and measurement repeatability are examined for the optimization of the geometry of the artefact. The results show that the developed 3D artefact is able to provide information of the volume occupied by the workpiece.

Keywords: ultra-precision machining, on-machine laser scanner, reconfigurable artefact, fiducial, volumetric errors, machine tools

1. Introduction

Multi-axis machine tools are key equipment in advanced industries for manufacturing complex freeform components, especially for ultra-precision diamond turning and polishing fields. The accuracy of the workpiece is significantly influenced by the geometric error of these machines. These errors have integrated effects in the manufacture of the products. The modelling and measurement of these volumetric errors are prime important in the high precision machine tools. As a result, it is recommended to regularly verify the accuracy of the machine tools [1, 2]. In order to improve the machining accuracy and efficiency, many approaches have been reported to measure and compensate the geometric error [2-4].

In the development of the error model, the homogeneous transformation matrix (HTM) [5] method is the commonly used. Other corresponding approaches have also been proposed such as Denavit-Hartenberg(D-H) transformation matrix [6], the screw theory [7, 8] and the differentiable manifold-based method [4]. For the identification of the geometric errors, the laser interferometer [9, 10] is the most popular measuring device to directly measure the error of the translational axes due to its high accuracy. However, this method is time-consuming

due to the repeatable process of adjusting the laser path before every measuring task. Laser ball bar and tracker [11-13] are also used to measure the volumetric error in an indirect way. Those approaches can provide reach information for the evaluation of machine performance. However, it is interesting to note that they all need to bring special instruments into the machine, which thus adding specialised personnel and leading to low efficiency [14]. To address this problem, artefact is employed to improve the effectivity.

Bringmann et al.[15] developed a 2D ball plate which can form a 3D working volume by moving the plate in a three-axis machine tool. Mayer [16] probed a scale enriched reconfigurable uncalibrated master ball artefact with the on-machine measuring system to separate the setup errors with the volumetric error of a five-axis machine tool. In addition, a ball dome artefact consisting of 25 precision balls was also fabricated [17] to check the performance of a multi-axis machine tool. These studies are performed on a high precision machine tool for checking the whole volumetric errors of the machine. Most of these methods can only achieve the accuracy at several micrometres and they focused on the whole volumetric errors of the machine tool which is not applicable for precision manufacturing freeform optics in a specific volume of the ultra-precision machine tool.

As a result, a reconfigurable fiducial-aided 3D artefact which takes the advantages of the characteristics of the machined workpiece into consideration is purposely designed in this study. Uncertainties including the gravity effect and measurement repeatability are examined to optimize the reconfigurable artefact. Hence, the HTM is employed to generate the kinematics model of a five-axis machine tool. An integrated on-machine measuring system is developed to evaluate the working volumetric errors in the machining process.

2. Research Methodology

2.1 Reconfigurable fiducial-aided positioning system design

The fiducial-aided calibrating and positioning artefact is not only designed to explore its capacity of positioning freeform surfaces in the manufacturing cycle, including manufacture, measurement and evaluation, but also identify the errors (i.e. geometric volumetric errors) of the corresponding machine tool. As a result, the designed reconfigurable fiducial-aided model should well suit the machining and measuring conditions, such as the working space, machine kinematics, tool collision and clamping. Standard balls are good fiducials because their positions can be easily acquired by many touch probe based on-machine CNC measurement instrument.

The basic idea is that the design of a workpiece fixture shaped with cuboid or cylinder which is capable of easily clamped in the machines. The balls bar is then assembled by a ball and a rod are mounted surrounding the workpiece with different heights so that a 3D space enveloping the machining work volume is established. The idea behind the variable heights of the balls is that the richer information on the working space of the machines can be gathered as well as achieving additional geometric constraints. It is clear that the ability for reconfiguration depending to the working environment (i.e. machine tools, workpiece) is the most important features of the new fiducial-aided design. It is noted that this characteristic provides the possibility of obtaining specific information in the desired areas. It has the ability to overcome the drawbacks of existing ones that require special fixtures for different workpiece as well as requiring additional equipment. Moreover, the fiducials such as standard balls can also calibrate the measuring systems. Once the fiducial aided positioning

system is established, there is no need for any manual operation to align the workpiece on the machine tool since the fiducials can provide the coordinate information.

The key requirement of the design is the stability of the artefact geometry in the measuring process. Thermal sensitivity due to working temperature and elastic deformation under different gravitational directions are considered as the main factors which should be minimized. In order to limit the thermal expansion and deflection, the ball is made of Si_3N_4. The fixture and the rods are made of steel. Moreover, some short stems made of steel are used to add the height of the ball bars to control the deformation. Thermally controlled environment is always necessary in the current experiments. As for the gravitational effect, it can be calibrated on a CMM by rotating the fixture to change the direction of the gravity in the process of calibration of the positions of the fiducials and the details are shown in the following section.

Figure 1 shows an example of the designed system consisted of five fiducials (N=5) mounted on a square fixture on a five-axis fly-cutting raster milling machine tool. There were five fiducials (standard spheres) that were designed surrounding the workpiece in the 3D artefact. The heights of the sphere were 20, 25 and 35 mm, and the distribution of these fiducials were also shown in Fig. 2.

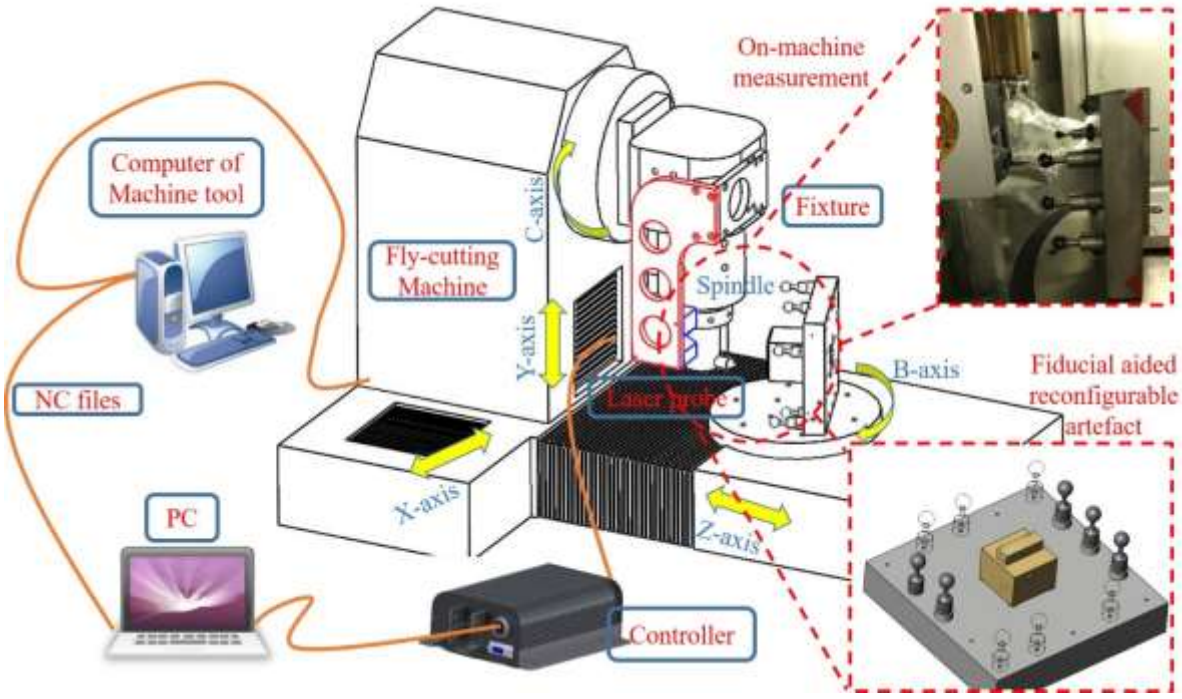

Fig. 1 A schematic diagram of the fiducial-aided reconfigurable artefact mounted on the B-axis of a five-axis ultra-precision machine tool.

2.2 Gravity effect on 3D artefact

In order to quantify the deviation resulting from the gravity (g), three expected positions are measured as shown in Fig. 2. One position is the horizontal position (H) that means the mounted ball bar plane of the fixture is parallel to the horizontal plane which is used for reference position as 0 ° position. The second position is vertical position (V) that is perpendicular to the horizontal plane as 90° position. The third position is 10° positions (O) from horizontal position. The unit of the artefact is mm.

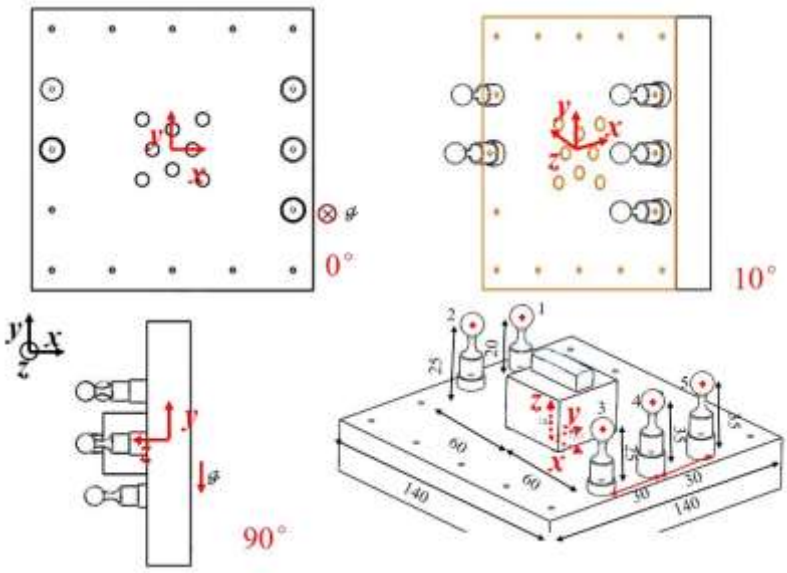

Fig. 2 The five fiducial aided 3D artefact measured in different positions

The deviations of the two positions including the three dimensions are achieved by the following equations:

$$\begin{aligned}
&\Delta x_{i,KH} = \bar{x}_{i,K} - \bar{x}_{i,H}, \Delta\bar{x}_{KH} = \frac{1}{N}\sum_{i=1}^{N} \| \Delta x_{i,KH} \| \\
&\Delta y_{i,KH} = \bar{y}_{i,K} - \bar{y}_{i,H}, \Delta\bar{y}_{KH} = \frac{1}{N}\sum_{i=1}^{N} \| \Delta y_{i,KH} \| \\
&\Delta z_{i,KH} = \bar{z}_{i,K} - \bar{z}_{i,H}, \Delta\bar{z}_{KH} = \frac{1}{N}\sum_{i=1}^{N} \| \Delta z_{i,KH} \| \\
&K = V, O; i = 1, 2\mathrm{K}\ N
\end{aligned} \tag{1}$$

$$\begin{aligned}
&\Delta d_{i,(x,y,z),KH} = \sqrt{(\Delta x_{i,KH})^2 + (\Delta y_{i,KH})^2 + (\Delta z_{i,KH})^2} \\
&\Delta\bar{d}_{(x,y,z),KH} = \frac{1}{N}\sum_{i=1}^{N} \Delta d_{i,(x,y,z),KH}
\end{aligned} \tag{2}$$

where $\bar{x}$, $\bar{y}$, $\bar{z}$ are the mean sphere centre coordinate with repeating measurement 3 times. $\Delta d_{i,(x,y,z),KH}$ is the total position variation of the *i*th sphere.

The effect of the gravity is measured and discussion in Section 3.1.

2.3 Probing fiducials with the on-machine measurement system

In this study, a five-axis ultra-precision machine tool incorporated with the developed on-machine measurement system as shown in Fig. 1, is used to evaluate the working volumetric error with the fiducial-aided artefact. The positions of fiducials in the artefact are provided by using the probing system for each re-localisation of the artefact. A total of 30 points in a 6 mm × 6 mm area are sampled uniformly on one standard sphere to guarantee its centre position using least square method. The calibrated diameter of the spherical fiducial was 9.997 mm. Figure 3 illustrates the probing directions.

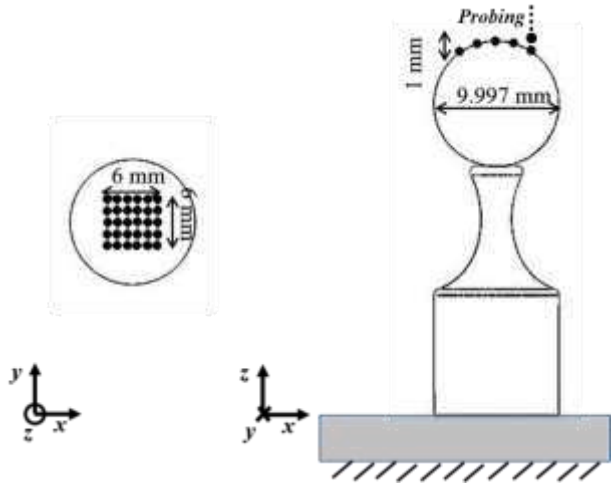

Fig. 3 Probing points on the standard sphere (left: *z* view; Right: *y* view)

The repeatability of measurement of the integrated probing system is evaluated by probing a standard sphere three times. The Cartesian repeatability ranges donated by the pooled standard deviation are 0.36 μm, 0.41 μm and 0.25 μm [18] respectively. In addition, the best fitted standard deviations of the sphere centres coordinates are 0.18 μm, 0.21 μm and 0.24 μm, respectively.

2.4 Machine tool kinematic model

The fiducial is used to obtain the probing information containing both errors resulting from the integrated on-machine measurement system and the machine tool itself. The relationship between the tip of the probe and tip of tool has been established in the previous work of the authors [18] . As mentioned earlier, the repeatability of measurement of the probing system is relatively low at 0.24 μm. It is reasonable to assume that the main contributor of the error sources is the machine tool. As a result, the integrated error effect can be synthesized to find the difference between the actual position and probing position of each fiducial in the working volume. It is not necessary to measure and model all the error separately. More attention should be focused on the synthesized influence of the measurement task. In the present work, the position errors of the fiducials are mainly considered. The ultra-precision raster milling machine tool has a wBZfXYCt topology as shown in Fig. 4.

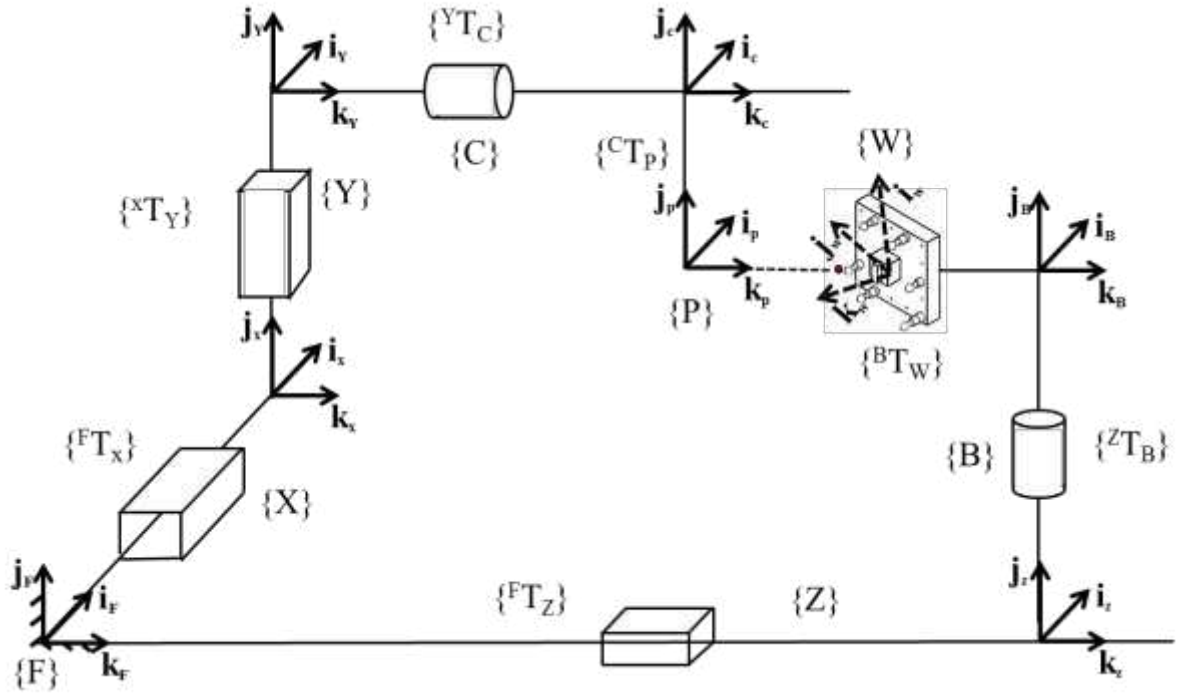

Fig. 4 Topological construction of the five-axis ultra-precision fly-cutting machine tool

The homogenous transformation matrix described in Eq. (3) is a powerful approach to connect the positions of the fiducials in different coordinates and each single error can be synthesized as a volumetric error.

$$ {}^{j}T_i = \begin{bmatrix} {}^{j}R_i & {}^{j}m_i \\ 0_{1\times3} & 1 \end{bmatrix} \tag{3} $$

${}^{j}T_i$ is a 4×4 homogenous transformation matrix which describes the coordinate transformation from the coordinate frame i to coordinate frame j . ${}^{j}R_i$ and ${}^{j}m_i$ stand for the rotation matrix (3×3) and the translation column vector (3×1), respectively.

The workpiece and tool branches of the machine tool are determined as follows:

$$ {}^{F}T_p = {}^{F}T_X \cdot {}^{X}T_Y \cdot {}^{Y}T_C \cdot {}^{C}T_P \tag{4} $$

$$ {}^{F}T_w = {}^{F}T_Z \cdot {}^{Z}T_B \cdot {}^{B}T_w \tag{5} $$

with the four tool branch sub-matrices are shown as follows:

$$ {}^{F}T_X = \begin{bmatrix} & x \\ I_{3\times3} & 0 \\ & 0 \\ 0_{1\times3} & 1 \end{bmatrix} \tag{6} $$

$$ {}^{X}T_Y = \begin{bmatrix} & 0 \\ I_{3\times3} & y \\ & 0 \\ 0_{1\times3} & 1 \end{bmatrix} \tag{7} $$

$$ {}^{Y}T_{C} = \begin{bmatrix} & & 0 \\ & R_C & 0 \\ & & 0 \\ 0_{1\times3} & & 1 \end{bmatrix} \quad R_C = \begin{bmatrix} \cos c & -\sin c & 0 \\ \sin c & \cos c & 0 \\ 0 & 0 & 1 \end{bmatrix} \tag{8} $$

$$ {}^{C}T_{P} = \begin{bmatrix} & & p_x + \Delta_{px} \\ & I_{3\times3} & p_y + \Delta_{py} \\ & & p_z + \Delta_{pz} \\ 0_{1\times3} & & 1 \end{bmatrix} \tag{9} $$

$$ {}^{F}T_{P} = \begin{bmatrix} & & x + R_C(p_x + \Delta_{px}) \\ & R_C & y + R_C(p_y + \Delta_{py}) \\ & & R_C(p_z + \Delta_{pz}) \\ 0_{1\times3} & & 1 \end{bmatrix} \tag{10} $$

The three workpiece branch sub-matrices are given as follows:

$$ {}^{F}T_{Z} = \begin{bmatrix} & & 0 \\ & I_{3\times3} & 0 \\ & & z \\ 0_{1\times3} & & 1 \end{bmatrix} \tag{11} $$

$$ {}^{Z}T_{B} = \begin{bmatrix} & & 0 \\ & R_B & 0 \\ & & 0 \\ 0_{1\times3} & & 1 \end{bmatrix} \quad R_B = \begin{bmatrix} \cos b & 0 & \sin b \\ 0 & 1 & 0 \\ -\sin b & 0 & \cos b \end{bmatrix} \tag{12} $$

$$ {}^{B}T_{w} = \begin{bmatrix} & & w_{i,x} + \Delta_{wix} \\ & R_w & w_{i,y} + \Delta_{wiy} \\ & & w_{i,z} + \Delta_{wiz} \\ 0_{1\times3} & & 1 \end{bmatrix} \tag{13} $$

$$ {}^{F}T_{w} = \begin{bmatrix} & & R_B(w_{i,x} + \Delta_{wix}) \\ & R_B & R_B(w_{i,y} + \Delta_{wiy}) \\ & & z + R_B(w_{i,z} + \Delta_{wiz}) \\ 0_{1\times3} & & 1 \end{bmatrix} \tag{14} $$

where the x, y, z, b and c are the machine axes positions for each fiducial. p_x, p_y and p_z are the probe centre coordinates and Δ_{px}, Δ_{py} and Δ_{pz} are the setup errors of the probe. ($w_{i,x}$, $w_{i,y}$, $w_{i,z}$) is the position of the ith fiducials relative to the last axis (B-axis) and Δ_{wix}, Δ_{wiy}, Δ_{wiz} are the fiducial i's setup errors. R_w is the rotation matrix and it is usually given as follows in most case of the studies.

$$ R_w = I_{3\times3} \tag{15} $$

Since there is no need to rotate the spindle in the probing process, the errors resulting from spindle are not included in the above equation model. It is noted that many commercial multi-axis machine tools are not equipped with on-machine probing system, which means the

developed on-machine probe may have different coordinate frame with that of the tool tip. Although the established fiducial-aided geometry is likely to minimize the impact of the error source in the measuring procedure, the transformation relationship has to be established before actual machining process.

The deviation between the probe tip centre and the *i*th fiducial is described as:

$$\delta_i - \begin{bmatrix} x \\ y \\ -z \end{bmatrix} - R_C \begin{bmatrix} p_x \\ p_y \\ p_z \end{bmatrix} + R_B \begin{bmatrix} w_{i,x} \\ w_{i,y} \\ w_{i,z} \end{bmatrix} = R_C \begin{bmatrix} \Delta_{px} \\ \Delta_{py} \\ \Delta_{pz} \end{bmatrix} - R_B \begin{bmatrix} \Delta_{wix} \\ \Delta_{wiy} \\ \Delta_{wiz} \end{bmatrix} \tag{16}$$

Assuming that the nominal values of the probe tips and fiducials have been estimated, all the error parameters can be treated as the following linear equation:

$$\mathbf{\Delta\delta} = J\mathbf{\Delta E} \tag{17}$$

where $\mathbf{\Delta\delta}$ is the deviation between the probe and the fiducials positions. J is the Jacobian matrix. $\mathbf{\Delta E}$ is the error vector including the probe and all the fiducials:

$$\mathbf{\Delta E} = [\Delta_{px}, \Delta_{py}, \Delta_{pz}, \Delta_{wix}, \Delta_{wiy}, \Delta_{wiz} \text{ L } \Delta_{wnx}, \Delta_{wny}, \Delta_{wnz}] \tag{18}$$

$$J = \begin{bmatrix} R_C & -R_B & 0_{3\times3} & \text{L} & 0_{3\times3} \\ R_C & 0_{3\times3} & -R_B & \text{L} & 0_{3\times3} \\ \text{M} & \text{M} & \text{M} & \text{O} & \text{M} \\ I_{3\times3} & 0_{3\times3} & 0_{3\times3} & \text{L} & -R_B \end{bmatrix} \tag{19}$$

The measuring results obtained from the probe and the calibrated artefact geometry are used to access the error parameters using the following system:

$$\mathbf{\Delta F} = J\mathbf{\Delta E} \tag{20}$$

where $\mathbf{\Delta F}$ denotes the difference between the on-machine measurement results and the calculated positions.

3. Experiments and discussions

3.1 Measurement of the gravity effect

For the five-axis machine tool, the artefact may be mounted in different orientation so that the orientation of the local gravity of the artefact may alter relative to the global gravity. As a result, three positions are measured. The position deviations are summarised by using the differences between the two tilt positon (10°, 90°) and the horizontal position (0°).

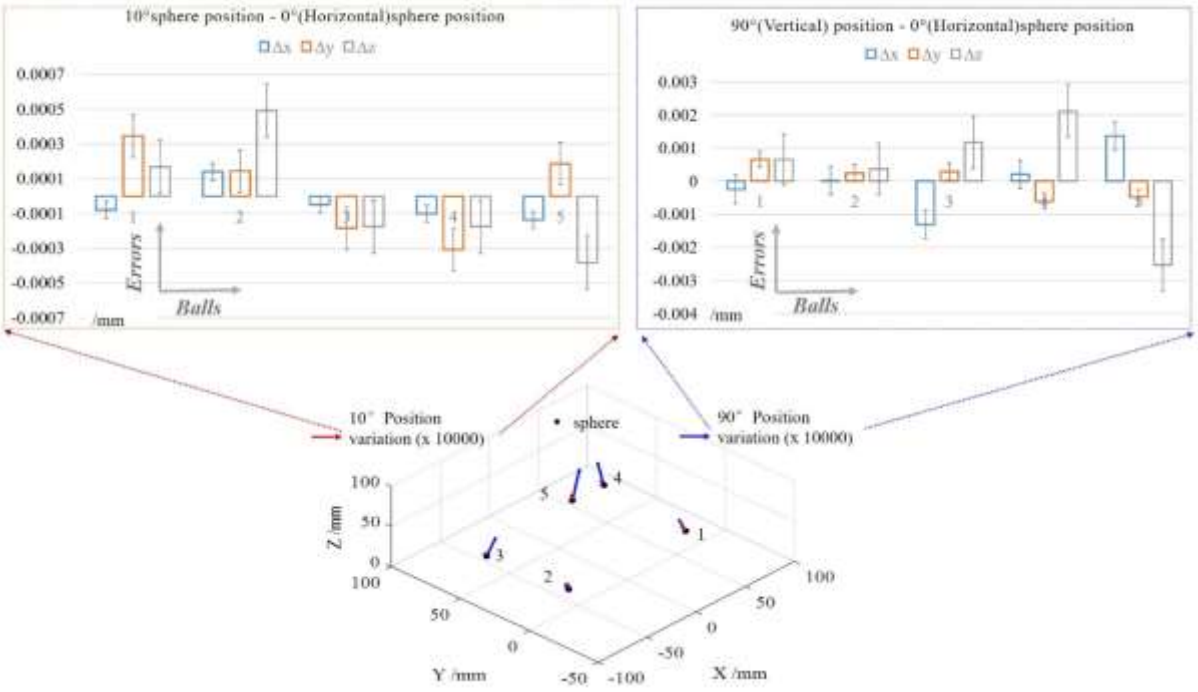

Fig. 5 Position deviations of the fiducials when changing artefact from a horizontal to a 10 degree (*O-H*) and to a vertical orientation (*V-H*). The errors vectors are multiplied by 10000 in the bottom plot. The top two graphs are position deviations in three directions with their uncertainties.

As shown in Fig. 5, the position variations go up when the angle of the artefact increases from the horizontal orientation. Position deviations are mainly below 1 μm in all directions but for fiducials which heights were more than 25 mm could be large to a few micrometres when the artefact rotated to the vertical position. It is noted that the position deviation in z direction (global coordinate frame in Fig.2) seems to be sensitive to the artefact rotation. This is because the component used to connect the fiducials to the fixture has deformation. The longer the component is, the more obvious the gravitational deformation is. The largest deviation reaches to $\Delta d_{5,VH}$ = 2.9 μm and $\Delta z_{5,VH}$ = 2.1 μm in total direction and z direction, respectively when the gravity orientation is changed from –*z* to –*y* for the local coordinate frame.

In this study, the effect caused by gravitational deformation is still needed to be considered although it is as small as several micrometres. As shown in Fig. 5, the results indicate that there are two facts which can be considered to reduce the effect. It is necessary to optimise the length of the connection component as short as possible with consideration of the working volume. In other words, it is helpful to add stiffness of the artefact. The other is that the artefact can be measured in a stable position in each measurement. For example, it is better to carry out the metrology in a horizontal position (0°) as shown in Fig. 2 in every measurement instrument. In this case, the measurement repeatability should be guaranteed in a particular position. Taking these two points into consideration, the height of each fiducial (z value as shown in Fig. 2 and Fig. 3) is controlled within 25 mm and the artefact was clamped in a vertical position in every measurement process and instrument, the raster milling machine tool and the coordinate measuring machine are used in this case. The deformations due to

weight are finally controlled in an acceptable level, the largest deformations are $\Delta\bar{z} \le 0.3\,\mu m$ and $\Delta\bar{d}_{(x,y,z)} \le 0.45\,\mu m$, respectively.

3.2 On-machine measurement

To determine the volumetric error of the five-axis horizontal machine with wBZfXYCt topology as shown in Fig. 1, a five standard sphere artefact is purposely designed as shown in Fig. 2 with variation of the height of each fiducial. Each calibrated centre position of the fiducial is listed in Table 1.

Table 1 Centre positions of the fiducials

Ball	X (mm)	Y (mm)	Z (mm)
1	59.31108	-0.25560	14.99509
2	-58.74790	0.864597	14.29131
3	-59.13960	59.79868	19.31120
4	59.49720	59.29094	24.40756
5	28.48006	59.94329	24.75141

In order to reduce the thermal effect to the fixture, the designed artefact is transformed and kept in a thermal controlled environment and they are measured by the on-machine probing system. According to the on-machine measurement system, the artefact was clamped in the vertical position on the B-axis as shown in Fig. 1. A number of tests were carried out by gradually increasing the rotary B- and C-axis in the measurement process. All the fiducials are probed to establish their centre coordinates and the positions (x, y, z, b and c) of the corresponding axes are also recorded. Considering the working volume of the measurement and machining conditions, a total number of 165 standard sphere centres were measured at the locations: b=0°, c=0°; b=0°, c=±5°; b=±5°, c=0°; b=±10°, c=0°;b=±5,c=±5 repeated three times in about two hours.

As shown in Fig. 6, the fiducial centre distances in a five fiducials artefact were compared with the distances in the fiducial aided CAD (calibrated fiducials and the CAD of the designed surface [18]) by using the cloud point fitting algorithm. The tested positions of the fiducials are determined and transferred into a common frame using mathematic model. Table 2 shows the compared results including the maximum value (r_{max}) and average values (r_{avg}) in a total of 10 distances in the artefact under different angular positions of the rotary axes. The r was defined in Fig. 6.

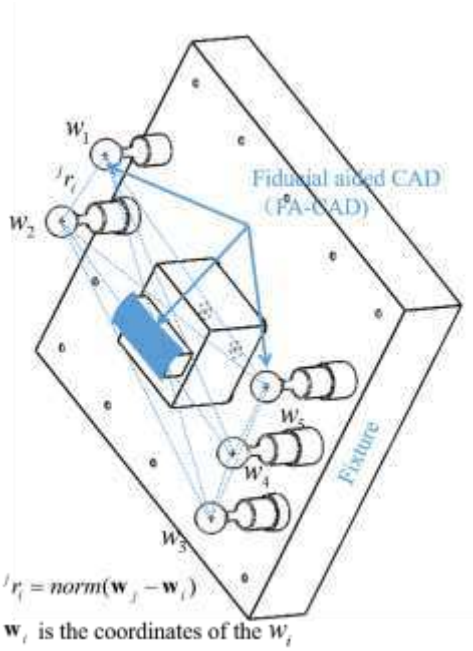

Fig. 6 Geometry definition of a five standard sphere artefact

As shown in Table 2, in the measured columns, it is clear that the deviations are lest, 0.9 μm at most when the measuring process are carried out with no rotation of the axes, which means that only three linear axes are used to perform the measurement. For setting the B-axis to 0°, the error is increasing with increasing angular positions of C-axis and reached to 6.5 μm. In this case, the volumetric errors resulting from the linear axes and errors from C axis are integrated into a fiducial when changing the position of the C-axis. It is interesting to note that the error only reaches to 6.8 μm when both of angular positions of the rotary axes are combined. Results in the mathematical model suggest that the errors are slightly smaller than those in the measured datasets. This is due to the existing setup errors of the integrated measuring system.

Table 2 Error of fiducial distances compared with the datasets in FACAD when using measured results and mathematic model under different rotary axes angular

Position of the rotary axes		①Measured (μm)		②Mathematic model (μm)		①-② (μm)	
b	c	r_{max}	r_{avg}	r_{max}	r_{avg}	r_{max}	r_{avg}
0°	0°	0.9	0.4	0.8	0.4	0.1	0.0
0°	5°	5.5	1.3	5.1	1.2	0.4	0.1
0°	-5°	5.4	1.1	5.3	1.1	0.1	0.0
5°	0°	1.1	0.6	0.8	0.4	0.3	0.2
5°	5°	5.6	1.6	5.5	1.5	0.1	0.1
5°	-5°	5.7	1.4	5.4	1.5	0.3	-0.1
10°	0°	1.6	0.6	1.3	0.8	0.3	-0.2
10°	5°	6.8	2.3	6.2	2.0	0.6	0.3
10°	-5°	6.4	2.2	6.1	1.8	0.3	0.4

Notes: ①, Measured value minus that in FACAD; ②, Mathematic model value minus that in FACAD

In addition, the residuals of the fiducials after best fitting to those calibrated in CMM were illustrated in Table 3. The results show that the maximum residual of the sphere diameters is up to 1 μm.

Table 3 The sphere diameters deviations

	x (μm)	y (μm)	z (μm)
Sphere 1	0.4	0.9	0.2
Sphere 2	0.5	0.8	0.4
Sphere 3	0.7	0.8	0.3
Sphere 4	0.7	1.0	0.3
Sphere 5	0.6	0.7	0.2

4. Conclusion

In this paper, a fiducial aided configurable artefact was proposed to evaluate volumetric error of a five-axis ultra-precision raster milling machine tool with an on-machine probing system. The 3D artefact allows the flexibility in the number and position of the fiducials according to the characteristics of the machine tool. A mathematical model is established to obtain the volumetric errors from the probing results. Measurement repeatability of the on-machine probing system is estimated at 0.24 μm. A detailed analysis of the effect of deflection due to gravity by tilting the artefact from a horizontal to a vertical orientation indicates that the stable orientation of the artefact and the length of connecting fiducial components which is as short as 25 mm could further reduce the errors of the artefact itself. Experiments are carried out by a 3D artefact consisting of five standard spheres on a five axis machine tool with wBZfXYCt topology. The distance method is employed in the estimation of the volumetric error by comparing the measured results and calculated values with those in the generated FA-CAD on a high precision CMM. When using the three linear axes, the maximum error is only 0.9 μm. This value slightly increases to 1.6 μm when the rotary B-axis is used. However, when both information of the rotary axes are associated, the worst error could sharply increase to 6.8 μm. Comparing with those values obtained in the mathematical model, it is found that the setup errors have a little contribution to the volumetric error in the measuring process. Those results show that the proposed 3D artefact possesses the ability of providing information of machine tool when a manufacturing process was carried out in the artefact envelop.

Declaration

a. Funding (information that explains whether and by whom the research was supported)
The work described in this paper was supported by National Key R&D Program of China (2017YFA0701200). The work was also supported by a grant from the Ministry of Science and Technology of China (Project Code: 2017YFE0191300). The authors would also like to express their thanks to the Research Office of The Hong Kong Polytechnic University (Project code: BBX7).

b. Conflicts of interest/Competing interests (include appropriate disclosures)
The authors have no conflicts of interest to declare that are relevant to the content of this article.

c. Availability of data and material (data transparency)

Not applicable

d. Code availability (software application or custom code)
Not applicable

e. Ethics approval (include appropriate approvals or waivers)
Not applicable

f. Consent to participate (include appropriate statements)
All authors agree to participate in this article.

g. Consent for publication (include appropriate statements)
All authors have read and agreed to the publication of the article.

h. Authors' contributions (optional: please review the submission guidelines from the journal whether statements are mandatory)
Shixiang Wang: Conceptualization, Methodology, Investigation, Validation, Data curation, Writing - original draft; Chi-Fai Cheung: Funding acquisition, Visualization; Resources, Supervision, Project administration; Writing - review& editing; Lingbao Kong: Investigation, Writing - review& editing.

References

[1] T. Liebrich, B. Bringmann, and W. Knapp, "Calibration of a 3D-ball plate," *Precision engineering,* vol. 33, pp. 1-6, 2009.

[2] S. Zhu, G. Ding, S. Qin, J. Lei, L. Zhuang, and K. Yan, "Integrated geometric error modeling, identification and compensation of CNC machine tools," *International journal of machine tools and manufacture,* vol. 52, pp. 24-29, 2012.

[3] "ISO230-1," in *Test code for machine tools Part 1: geometric accuracy of machines operating under no-load or quasi-static conditions*, ed, 2012.

[4] W. Tian, W. Gao, D. Zhang, and T. Huang, "A general approach for error modeling of machine tools," *International Journal of Machine Tools and Manufacture,* vol. 79, pp. 17-23, 2014.

[5] A. C. Okafor and Y. M. Ertekin, "Derivation of machine tool error models and error compensation procedure for three axes vertical machining center using rigid body kinematics," *International Journal of Machine Tools and Manufacture,* vol. 40, pp. 1199-1213, 2000.

[6] B. K. Jha and A. Kumar, "Analysis of geometric errors associated with five-axis machining centre in improving the quality of cam profile," *International Journal of Machine Tools and Manufacture,* vol. 43, pp. 629-636, 2003.

[7] J. Yang and Y. Altintas, "Generalized kinematics of five-axis serial machines with non-singular tool path generation," *International Journal of Machine Tools and Manufacture,* vol. 75, pp. 119-132, 2013.

[8] S. Xiang and Y. Altintas, "Modeling and compensation of volumetric errors for five-axis machine tools," *International Journal of Machine Tools and Manufacture,* vol. 101, pp. 65-78, 2016.

[9] S. Ibaraki and W. Knapp, "Indirect Measurement of Volumetric Accuracy for Three-Axis and Five-Axis Machine Tools: A Review," *Int. J. Automation Technol.,* vol. 6, pp. 110-124, 2012.

[10] A. Wan, L. Song, J. Xu, S. Liu, and K. Chen, "Calibration and compensation of machine tool volumetric error using a laser tracker," *International Journal of Machine Tools & Manufacture,* vol. 124, p. 126, 2018.

[11] S. Aguado, D. Samper, J. Santolaria, and J. J. Aguilar, "Identification strategy of error parameter in volumetric error compensation of machine tool based on laser tracker measurements," *International Journal of Machine Tools and Manufacture,* vol. 53, p. 160, 2012.

[12] M. Tsutsumi and A. Saito, "Identification and compensation of systematic deviations particular to 5-axis machining centers," *International Journal of Machine Tools and Manufacture,* vol. 43, pp. 771-780, 2003.

[13] S. H. H. Zargarbashi and J. R. R. Mayer, "Assessment of machine tool trunnion axis motion error, using magnetic double ball bar," *International Journal of Machine Tools and Manufacture,* vol. 46, pp. 1823-1834, 2006.

[14] T. Erkan, J. R. R. Mayer, and Y. Dupont, "Volumetric distortion assessment of a five-axis machine by probing a 3D reconfigurable uncalibrated master ball artefact," *Precision Engineering,* vol. 35, pp. 116-125, 2011.

[15] B. Bringmann, A. Küng, and W. Knapp, "A Measuring Artefact for true 3D Machine Testing and Calibration," *CIRP Annals - Manufacturing Technology,* vol. 54, pp. 471-474, 2005.

[16] J. R. R. Mayer, "Five-axis machine tool calibration by probing a scale enriched reconfigurable uncalibrated master balls artefact," *CIRP Annals - Manufacturing Technology,* vol. 61, pp. 515-518, 2012.

[17] J. R. R. Mayer and H. Hashemiboroujeni, "A ball dome artefact for coordinate metrology performance evaluation of a five axis machine tool," *CIRP Annals - Manufacturing Technology,* vol. 66, pp. 479-482, 2017.

[18] S. Wang, C. Cheung, M. Ren, and M. Liu, "Fiducial-aided on-machine positioning method for precision manufacturing of optical freeform surfaces," *Optics express,* vol. 26, pp. 18928-18943, 2018.